



assure more stable operation. The half bandwidth was extended from 210 Hz in an optimum coupling to 325 Hz, and the increase of the required input rf power is about 5% in this case. The optimum structure of a coaxial rf window with a planar ceramic disk, a doorknob transition to a waveguide system and a pair of coupling waveguide as a vacuum chamber was determined with the HFSS code, as shown in Fig. 3 and Fig. 4. The maximum electric field of 770 kV/mm at the rf window is estimated at input power of 350 kW.

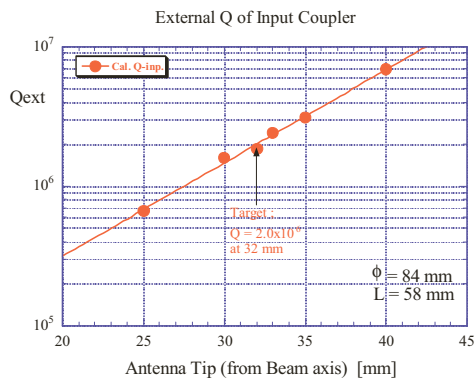


Figure 2: Calculated external Q value as a function of the antenna tip position from the beam axis. ( $\phi$  is a diameter of the beam tube, 84 mm, and L is a length between the cell-end and the antenna axis, 58 mm)

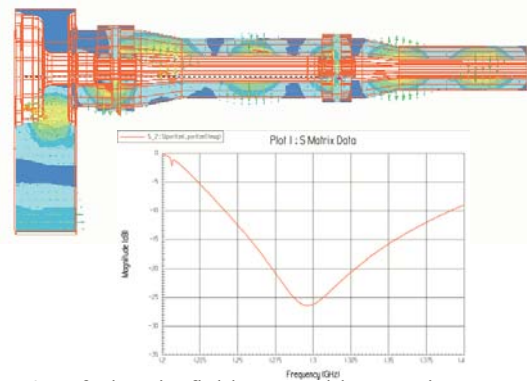


Figure 3: Rf electric field at a cold-warm input coupler and a doorknob, and the frequency characteristics ; (S11 = -26.2 dB at 1.3 GHz,  $\epsilon^*$  of ceramic = 9.2).

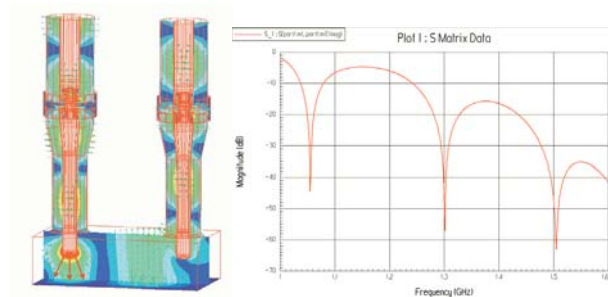


Figure 4: Rf electric field at a coupling waveguide and two cold couplers, and the frequency characteristics ; (S11 = -55. dB at 1.3 GHz,  $\epsilon^*$  of ceramic = 9.2).

## FABRICATION OF INPUT COUPLERS

### RF windows

Ceramics disks are made of  $Al_2O_3$  with the purity of 95%, (HA95 from NTK). The disk sizes of a cold and a warm rf window are 6.2 mm and 6.6 mm in the thickness, 92 mm and 116 mm in the outer diameter, respectively. Thermal shock tests of the ceramics disks were repeatedly carried out by liquid nitrogen. After this, coating with TiN on the surface of the vacuum side was performed, and the thickness of the deposited layer is about 10 nm. First brazing for fabricating rf windows was carried out at about 1000 °C in a hydrogen furnace, and the completed coaxial rf windows are shown in Fig. 5, (at Toshiba ETD).

### Input Couplers

The second step of the brazing procedure is the joining of rf windows and coaxial parts which consist of an inner conductor (antenna) and an outer conductor. The coaxial parts are made of stainless steel, and copper plating of 30  $\mu$ m on the rf surface was carried out, except an outer conductor of a cold coupler (5  $\mu$ m) to reduce a heat transfer. The completed couplers after the second brazing at about 800 °C are shown in Fig. 6. In the final step, small flanges made of stainless steel were welded with the ports by TIG.



Figure 5: Two warm rf windows (Top) and two cold rf windows (Bottom) after the initial brazing.



Figure 6: Four cold couplers (Top) and two warm couplers (Bottom) after the final brazing.

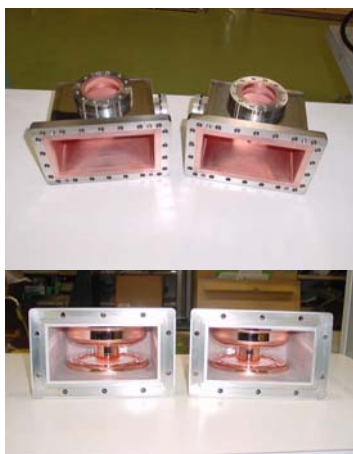


Figure 7: Coupling waveguides for a vacuum chamber (Top) and two door-knob-type transitions (Bottom).

### Door-knob Transitions

A door-knob, as shown in Fig. 7 (Bottom), is used for transition between a coaxial line (104D) and a waveguide system (WR650). The inner component like a door-knob-shape was formed by spinning from a thin copper plate of 0.6 mm and was fixed with the outer frame made of aluminium. The location of an end-plate for a short circuit of a waveguide was adjusted before welding, so as to make a matching condition best at 1.3 GHz.

### Coupling Waveguides

A pair of coupling waveguide, as shown in Fig. 7 (Top), is used for a vacuum chamber to install a pair of input couplers. The coupling waveguide was fabricated with stainless steel plates of 5 mm, and the inner surface was coated with copper plating of 30  $\mu\text{m}$  to suppress heating due to rf losses. Two facing flanges were joined with an indium seal.

## HIGH POWER TEST STAND

### Assembling Procedure

Components of the input couplers and the coupling waveguides were carefully rinsed with ultra-pure water at nominal pressure, and were dried for one day in a clean room (class 10), as shown in Fig. 8. After assembling of the input coupler system in a clean room, pumping was carried out by two vacuum systems composed of a turbo molecular pump of 320 l/s and a scroll pump of 250 l/m; one is for the cold coupler side including the coupling waveguide, and another is for two warm couplers. The input coupler system was bake out at 100 °C for 48 hours, prior to rf processing. The vacuum pressure at room temperature reached to less than  $10^{-5}$  Pa.

### RF Measurement

Rf characteristics of the whole input coupler system for high power tests were measured, as shown in Fig. 9. Reflection is less than about -20 dB within the wide range of 70 MHz. Reflected power of about 1 % was confirmed in an operation at 1.3 GHz.

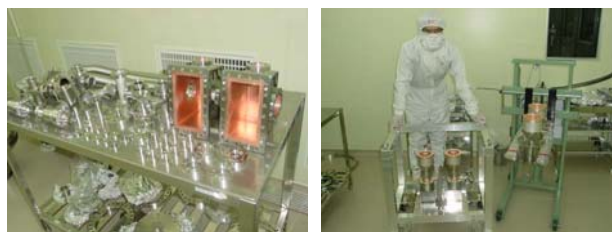


Figure 8: Assembly of the input couplers in a clean room.

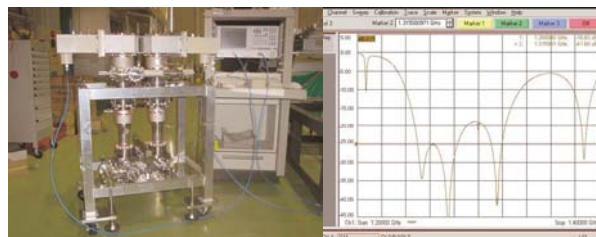


Figure 9: RF measurement of the whole system of the test stand, ( $S_{11} = -18.8$  dB at 1.3 GHz).

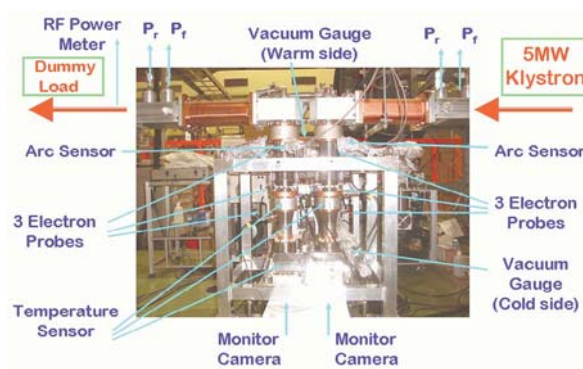


Figure 10: Se-up of the high power test stand.

### High Power Test System

An experimental set-up for high power tests is shown in Fig. 10. A pulsed klystron with the maximum output rf power of 5 MW in an operation with 1.5 msec and 5 Hz is used for the high power tests. The waveguide system is connected with a 5 MW circulator and terminated by a water-cooled dummy load. Forward and reflected rf powers are monitored by two directional couplers connected at both the up-stream and the down-stream of the test stand. An ionization vacuum gauge is installed in each pumping system of the cold coupler side and the warm coupler side. An arc sensor is attached at the vacuum side of each rf warm window. Three electron pick-up probes in each coupler are attached at the location close to both sides of the cold rf window and only vacuum side of the warm rf window. Temperature rises at the rf windows are monitored by thermal sensors. Two video cameras at the bottom of the coupling waveguides can observe visible lights like a glow discharge by multipacting. These monitoring instruments are very important to prevent a fatal sparking discharge around the rf windows.

## RF PROCESSING AT TEST STAND

### Processing of #1 and #2 Input Couplers

Rf processing was initially started in a 100  $\mu$ sec and 1 Hz operation. The first deterioration of the vacuum pressure was observed at 40 kW in the cold side and at 70 kW in the warm side. Interlock level of the vacuum pressure was set to  $7 \times 10^{-4}$  Pa in the initial processing, and then reduced to  $2 \times 10^{-4}$  Pa. The rf processing procedure was carried out very carefully, so that the processing time was 13 hours up to 300 kW and 22 hours up to 1 MW, as shown in Fig. 11. After this, the repetition rate was increased to 5 Hz, and no severe vacuum deterioration was observed with the increase of the rf power. The power supply system of the klystron was improved in order to extend an available pulse width from 100  $\mu$ sec to 1.5 msec. The second run of rf processing was carried out up to 1.4 MW in a 100  $\mu$ sec and 500  $\mu$ sec operation with 5 Hz, and finally the rf power of 1.0 MW in a 1.5 msec operation was successfully transferred to the input couplers.

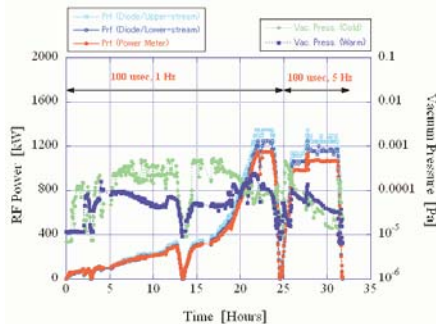


Figure 11: Time evolution of the input rf power and the vacuum pressure during the initial rf processing in a 100  $\mu$ sec and 1 Hz operation for the #1 and #2 couplers.

### Processing of #3 and #4 Input Couplers

Initial rf processing was started in a shorter pulse width of a 10  $\mu$ sec and 5 Hz operation, and the processing time up to 1.9 MW was about 20 hours, as shown in Fig.12. Then, the pulse width was extended to 30  $\mu$ sec, 100  $\mu$ sec and 500  $\mu$ sec, and finally processing up to 1.0 MW in a 1.5 msec and 5 Hz operation was carried out without any problem. The total processing time was about 50 hours and is summarised in Fig.13.

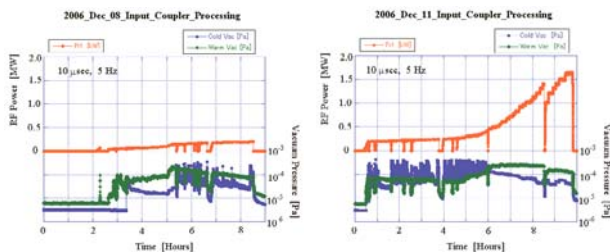


Figure 12: Time evolution of the input rf power and the vacuum pressure during the initial rf processing in a 10  $\mu$ sec and 5 Hz operation for the #3 and #4 couplers.

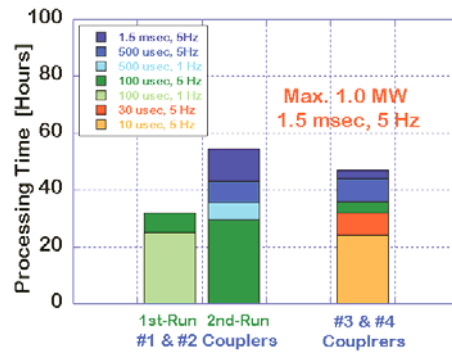


Figure 13: Total processing time up to 1.0 MW in a 1.5 msec and 5 Hz operation.

## ASSEMBLY OF CRYOMODULE

### Installation of a Cold Coupler in a Cavity

One cavity for the STF Phase-0.5 was assembled with a cold input coupler in a new clean room (class-10), as shown Fig. 14. The outside of the coupler was carefully cleaned by wiping and blowing. The inside of the couplers was filled by filtered high purity nitrogen gasses, just before dismounting from the test stand. A helicoflex seal coated with indium plating of 30  $\mu$ m and stainless steel bolts coated with silver plating were used for joining with the flange of the cavity port.



Figure 14: Installation of a cold coupler into a cavity

### Assembly of the Cryomodule

The cavity equipped with a cold input coupler and a tuner system was installed in a gas return pipe of one 6m-cryomodule, as shown in Fig. 15. A heater was attached surround a cold window with a thermal sensor for in-situ baking inside the cryomodule. Baking of a cold rf window prior to rf processing at room temperature is very effective to reduce the processing time. Since bellows at the cold input coupler were eliminated, the supporting system of the coupler is unnecessary and the installation work had been very simple and easy.



Figure 15: Baking heater and 80 K shielding attached on a cold rf window (Left), and an assembled cavity mounted on 2 K gas return pipe (Right).

## RF PROCESSING IN THE CRYOMODULE

### Installation of a Warm Coupler

After installation of the cryomodule in the STF tunnel, connection of a warm coupler with a cold coupler was carried out in a working area covered with a special clean booth to keep a clean environment, as shown in Fig.16. The cold rf window in a insulation vacuum of the cryomodule and the warm coupler pumping system were baked out at 100 °C for 65 hours, and the vacuum pressure in the cold (cavity) side and in the warm side reached to  $3 \times 10^{-7}$  Pa and  $7 \times 10^{-7}$  Pa at room temperature, respectively.



Figure 16: Installation of a warm coupler in a cryomodule.

### RF Processing in the Cryomodule

After baking, a doorknob transition was attached in the warm coupler and was connected with a 500 kW circulator by a flexible waveguide, as shown in Fig. 17. Rf processing in the cryomodule was started in a 30  $\mu$ sec and 5 Hz operation, and the input rf power reached to a target power of 230 kW within only 2 hours, as shown in Fig.18. No vacuum deterioration was observed in the cold (cavity) vacuum. Electron activities were detected only at the warm side of the cold window, and the multipacting level was observed around 100 kW. There was no work of the interlock system during keeping at 250 kW for 7 hours, except trivial troubles of the rf power source. Temperature at the cold window increased to 37 °C in the end of the rf processing. Rf processing at room temperature was carried out for total 23 hours in three days. The high gradient test of the cavity at 2 K is scheduled in November 2007, in the next step.

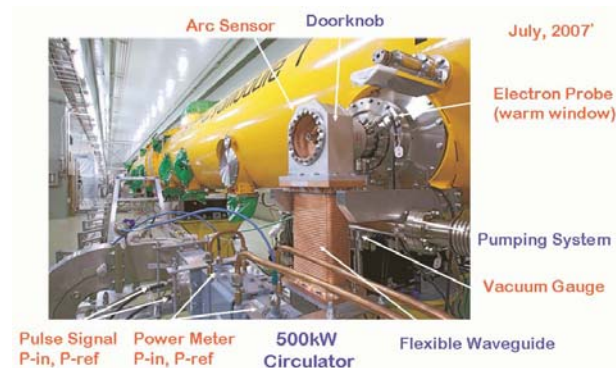


Figure 17: Set-up for the rf processing in the cryomodule.

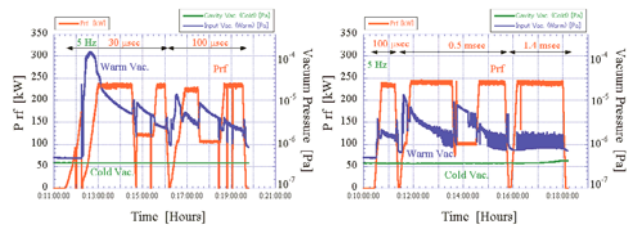


Figure 18: RF processing logs of one input coupler in the cryomodule at room temperature.

## SUMMARY

Four input couplers for the STF baseline cavity system were designed and fabricated. They had been successfully tested at the high power test stand up to 1.0 MW in the pulsed operation with 1.5 msec and 5 Hz. One coupler had been installed in the STF cryomodule, and had been processed up to 250 kW at room temperature. High power tests in the cryomodule to achieve a higher accelerating gradient at 2 K will be carried out soon.

## ACKNOWLEDGMENTS

The authors would like to thank A. Yano and K. Tetsuka (Toshiba Electron Tubes & Devices Co., Ltd.) for the fabrication of the input couplers. Special thanks are given to N. Okamoto (Broad Wireless Co., Ltd.) for manufacturing the doorknob transitions.

One of the authors, Eiji Kako, deeply appreciates Mr. Minoru Kawaguchi for his continued effort and hard work in the construction of the high power rf distribution system.

## REFERENCES

- [1] S. Noguchi, et al., "STF Baseline Cavities and RF Components", SRF2005, Cornell Univ., Ithaca, USA, (2005), <http://www.lns.cornell.edu/public/SRF2005/>. Also, presentation for the ILC seminar at KEK, (May 11<sup>th</sup>, 2007), <http://lcdev.kek.jp/LocalMeetings/>.
- [2] H. Hayano, "Superconducting RF Test Facility (STF) in KEK", SRF2005, Cornell Univ., Ithaca, NY, USA (2005) p409-411.
- [3] E. Kako, et al., "Construction of the STF Baseline Cavity System for STF at KEK", PAC07, Albuquerque, NM, USA, (2007) p2107-2109.
- [4] S. Noguchi, E. Kako and K. Kubo., "Couplers – Experience at KEK", 4<sup>th</sup> SRF Workshop, KEK, Tsukuba, Japan, (1989) p397-412.
- [5] E. Kako, S. Noguchi and T. Shishido, "Input Couplers for 972 MHz Superconducting Cavities in the High Intensity Proton Linac", 11<sup>th</sup> SRF Workshop (SRF2003), Luebeck/Travemuende, Germany, (2003) ThP27.